

Received March 22, 2019, accepted April 8, 2019, date of current version April 29, 2019.

Digital Object Identifier 10.1109/ACCESS.2019.2912183

Effect of Diamond Nanoparticle on the Friction Property of Sliding Friction Pair With Molecular Dynamics Simulation

WEIJIE SHI¹, HAIXIA ZHAO¹, AND XIAOHUI LUO²

¹College of Electromechanical Engineering, Qingdao University of Science and Technology, Qingdao 266061, China

²School of Mechanical Science and Engineering, Huazhong University of Science and Technology, Wuhan 430074, China

Corresponding author: Weijie Shi (weijieshi@qust.edu.cn)

This work was supported by the Youth Science Foundation of National Natural Science Foundation of China under Grant 51305146.

ABSTRACT Effect of the diamond nanoparticle on the friction property of the sliding friction pair is investigated using the molecular dynamics simulation. A molecular dynamics simulation model without the diamond nanoparticle is also set up. The simulation is conducted at an external load of 60 nN. The results confirm that adding diamond nanoparticle can improve the friction property. With increasing the diameter, the angular velocity, and the indentation depth decrease inversely. Also, when the diameter varies from 32.13 Å to 49.98 Å, the friction force, and the contact area are both inversely proportional to 3.6 power of the diameter. The relationship between friction force and contact area shows a linear increase law, which indicates that friction force is affected by the contact area.

INDEX TERMS Nanocontacts, friction, molecular computing.

I. INTRODUCTION

When two contact solids slid against each other, friction and wear will occur at the interface [1], [2]. Many researchers have investigated the friction characteristics of the nanoparticles lubricants and found that the nanoparticles can improve the friction property of lubricants. Kim *et al.* [3] added the diamond nanoparticles with diameter from 5 nm to 10 nm into the paraffin oil and conducted the friction test. They found that the diamond nanoparticles could improve the friction properties of paraffin oil, because the diamond nanoparticles were spherical particles and rolled between the friction pair. The nanoscale fluid friction test was carried out by Dennis *et al.* [4] at water lubricated with adding carbon microspheres. The results showed that the carbon microspheres played a role in ball bearings, and the friction coefficient was reduced by about 0.03. Chu *et al.* [5] added the diamond nanoparticles at diameter 4.37 nm into lubricating oil and prepared the nano fluid with concentration of 0%, 1%, 2% and 3%. By conducting the ring block friction and wear test, they found that the diamond nanoparticles can improve the tribological properties of lubricating oil. The

friction coefficient at volume fraction of 2% was the lowest and the wear loss was lowest at volume fraction of 3%. Novak *et al.* [6] studied the effect of concentration of diamond nanoparticles on the friction properties of paraffin oil. The diameter of diamond nanoparticles was 3-10 nm and the mass fraction was 0.5%, 1% and 2%. They found that the mass fraction of 1% paraffin oil had the most excellent friction properties and the coefficient of friction was reduced by 13%. Previous studies have suggested that the nanoparticles can play the role of the micro bearing when they are used as lubricant additives.

With the rapid improvement of computer calculating ability, MD simulation has been an important method to investigate the micro tribological behavior [7], [8]. Also, lots of researchers used the MD simulation to investigate the friction property of nanoparticles [9]–[15]. Lee *et al.* [9] performed a MD simulation to study the rolling characteristics of Ni spheres at the nanoscale. In the simulation, rigid Ni spheres with diameter of 6 nm and 12 nm used were rolled on a Cu substrate. Their results indicated that the smaller sphere showed a higher friction level and rolling depth greatly increased the rolling friction. Zhang and Tanaka [10] investigated the deformation of silicon monocrystals induced by three-body contact sliding with the aid of the MD analysis.

The associate editor coordinating the review of this manuscript and approving it for publication was Debashis De.

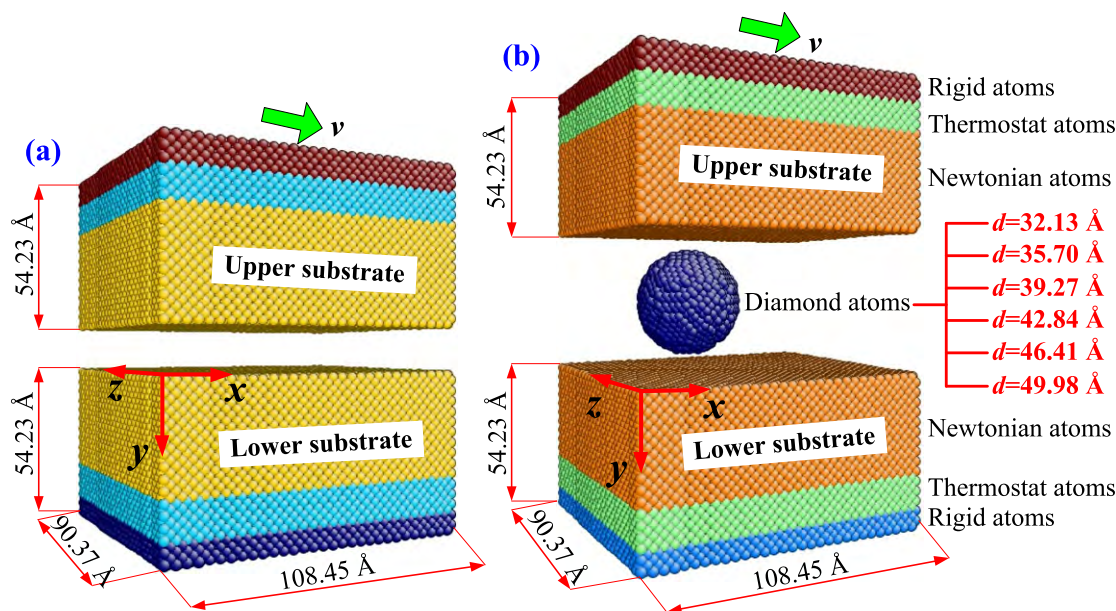


FIGURE 1. Friction model using the MD simulation: (a) sliding model without diamond nanoparticle and (b) rolling model with diamond nanoparticle.

Sun *et al.* [12] carried out a MD simulation to study the nanoscale three-body abrasion for the diamond-monocrystal silicon system. They found that there exists only the rolling movement of diamond nanoparticle and friction force is proportional to normal force in three-body abrasion model. Si *et al.* [13] investigated the effects of abrasive rolling on material removal and surface finish using MD simulation methods. They found that both abrasive rolling and sliding were important for the material removal.

In addition, working parameters which affect the friction property of nanoparticles, such as velocity [16], shape of nanoparticle [17], [18], temperature [19], [20] and normal load [21] have been well researched by the MD simulation. Hu *et al.* [16] studied the friction behaviors of silicon dioxide and diamond nanoparticle with MD simulations. The results showed that when velocity and load is low, the nanoparticle can act as bearings. However, when the load was increased, the rolling effect of silicon dioxide was loss. Shi *et al.* [17] investigated the influence of normal load and nanoparticle shape on the rolling friction property under low humidity conditions. They found that the movement pattern of nanoparticles can be changed from sliding to rolling by tuning the nanoparticle shape. Khomenko *et al.* [19] studied the friction properties of Pd and Al nanoparticles on a graphene surface and point out that the averaged friction force depends nearly linearly on the contact area and non-monotonously on the temperature.

However, there is still much uncertainty about the friction reduction mechanisms of nanoparticle. In order to further reveal how the addition of nanoparticle decrease the friction force, two MD simulation models with and without the diamond nanoparticle under dry condition are conducted in this paper. The relationship between the friction property and

the diameter is also investigated with the MD simulation to explain how the diameter of nanoparticle changes the friction force at the nanoscale.

II. COMPUTATIONAL SCHEME

In this section, the model setup, molecular dynamics and computational method are described.

A. MODEL SETUP

To build the friction model, LAMMPS [22] is used to conduct the MD simulation and AtomEye [23] is adopted to visualize the model. As shown in the Figure 1, two MD models are built to illustrate the friction property of diamond nanoparticle, including sliding model without diamond nanoparticle and rolling model with diamond nanoparticle. When no diamond nanoparticle is present, two substrates contact each other directly, which is described in Figure 1(a). The two substrates consist of upper substrate and lower substrate. Both upper substrate and lower substrate are the same size of $30a_c \times 15a_c \times 25a_c$, where is the lattice constant of copper (3.615 Å). They contain 47430 copper atoms, including 6120 rigid atoms, 10710 thermostat atoms and 30600 Newtonian atoms, respectively. The thicknesses of the rigid atoms and the thermostat atoms are 7.23 Å and 10.85 Å, respectively. In the simulation, periodic boundary conditions are adopted in the x and z directions.

In addition, a comparative analysis is conducted to investigate the friction properties of diamond nanoparticle by placing it between the upper substrate and the lower substrate, which is described in the Figure 1(b). The nanoparticle can move freely and no artificial external load is imposed. The dimensions and structures of the two substrates in the Figure 1 (b) are same with those in the Figure 1(a). Diamond

nanoparticles with different diameters (9 a_d , 10 a_d , 11 a_d , 12 a_d , 13 a_d and 14 a_d) are applied to study how the diameter affects the friction property, where a_d is the lattice constant of diamond, $a_d = 3.567 \text{ \AA}$. The corresponding numbers of the diamond nanoparticles are 3059, 4189, 5577, 7247, 9194 and 11509, respectively.

B. MOLECULAR DYNAMICS

In the simulation, the interaction between copper atoms is described by adopting the EAM potential [24]. The diamond nanoparticle is treated as the rigid and diamond-diamond interaction is ignored. The copper-diamond interaction is modeled by the Morse potential:

$$E = D_0[\exp^{-2\alpha(r-r_0)} - 2 \exp^{-\alpha(r-r_0)}] \quad (1)$$

where D_0 , is a parameter determined by the cohesive energy, α is the elastic modulus, r is the dynamic distance and r_0 is the equilibrium distance. In addition, the values of D_0 , α , r and r_0 are 0.087eV, 5.14, 2.05 \AA [25], [26].

Three steps, including relaxation step, indentation step and sliding step, are adopted to realize the MD simulation. During the relaxation step, the model is relaxed for 100 picoseconds (ps) and an equilibrium state is acquired. The canonical ensemble (NVT) is applied to the thermostat atoms and Newtonian atoms. Additionally, the rigid atoms are fixed to keep the model height unchanged. At the indentation step, an external load (60 nN) is imposed on the upper substrate along the position direction of y axis. The temperature of thermostat atoms is kept at 298 K by adopting the Langevin thermostat and the micro-canonical ensemble (NVE) is applied to the Newtonian atoms. The target external load is reached by gradually increasing the external load from 1, 6 and 30 nN to finally 60 nN during 80 ps. Because the external load is increased during the indentation step, sliding step is not adopted until the target external load of 60 nN is acquired. At the sliding step, the NVE is used for the Newtonian atoms of both substrates. The upper substrate moves at a constant velocity of 100 m/s along the positive direction of x axis. The sliding step is performed for 150 ps with time step equal to 0.001 ps.

C. COMPUTATIONAL METHOD

Defining the friction force, friction coefficient, indentation depth and contact area is significant in understanding the friction mechanism at the nanoscale. In the MD simulation, the diamond nanoparticle force acting on upper substrate (DFUS) and the diamond nanoparticle force acting on lower substrate (DFLS) are obtained by the LAMMPS. The friction force f and the normal force F_{ex} are calculated by averaging the DFUS and DFLS along the x and y direction, respectively. The friction coefficient is the friction force divided by the normal force

$$\mu = f/F_{ex} \quad (2)$$

Figure 2 illustrates the principle of indentation depth. The indentation depth is the average value of the indentation

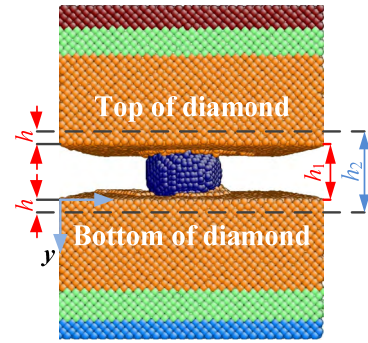


FIGURE 2. Definition of indentation depth.

depth of upper substrate and lower substrate, which can be calculated by

$$h_{id} = (h_1 - h_2) / 2 \quad (3)$$

where h_1 is the distance between the undisturbed interfaces of the upper substrate and the lower substrate, h_2 is the distance extension of diamond nanoparticle in the y direction.

In this study, the contact area is calculated by averaging that of the upper substrate and lower substrate with the diamond nanoparticle. When a diamond atom is in the range of chemical interactions of other copper atom, the diamond atom is called contact area [27]–[29]. Therefore, the contact area can be calculated by

$$A_{real} = N_{at}A_{at} / 2 \quad (4)$$

where N_{at} is the number of contact atoms, including the contact atom of upper substrate and lower substrate, A_{at} is average surface area per atom.

III. RESULTS AND DISCUSSION

The results and discussion section is divided into three sections: friction property analysis, effect of diameter on the indentation characteristic and effect of diameter on the friction property.

A. FRICTION PROPERTY ANALYSIS

Figure 3 shows the friction property of MD sliding simulations without the diamond nanoparticle at external load of 60 nN. From Figure 3(a), it can be seen that when the upper substrate begins to slide, the friction force will reach a high peak (577 nN) at 11 ps. This is because both the substrates lock each other. As the Figure 4 shows, the upper substrate and the lower substrate seem to perform a whole copper material at point A. When the sliding time is higher than 11 ps, the friction force will decrease rapidly and gradually stabilize at 101 nN. The friction morphology at point B is described in the Figure 4. It can be seen that the friction process tends to be stable and the upper and lower matrix are no longer locked. On the other hand, Figure 3(a) also shows the normal force at external load of 60 nN. The normal force rapidly increases firstly but decreases subsequently and reaches at 60 nN, which is identical to the external load.

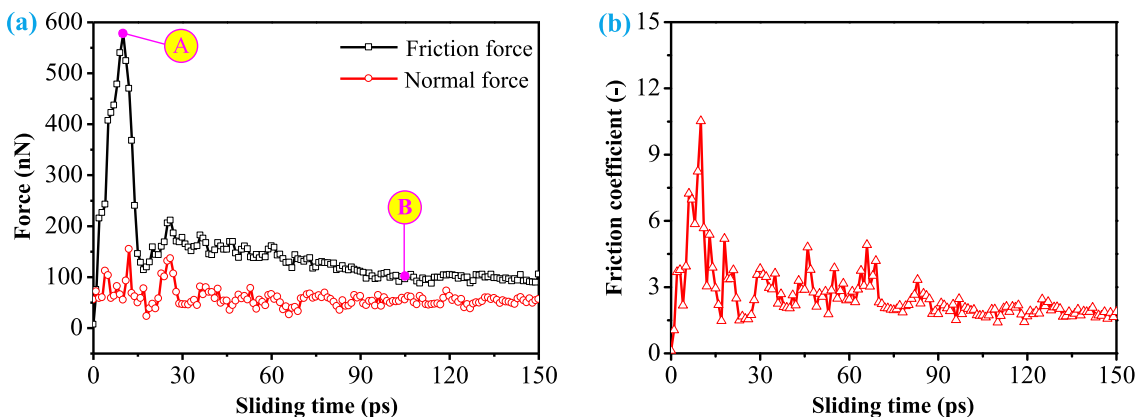


FIGURE 3. Friction property analysis for sliding model without diamond nanoparticle: (a) force and (b) friction coefficient.

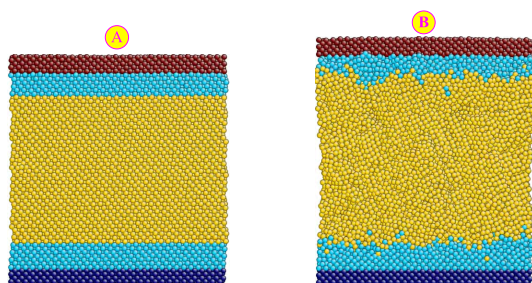


FIGURE 4. Friction morphologies for sliding model without diamond nanoparticle at sliding time of 11 ps (point A in Figure 3) and 105 ps (point B in Figure 3).

Additionally, Figure 3(b) illustrates the friction coefficient varying with the sliding time. The change in friction coefficient coincides well with the friction force. When the sliding time is at 11 ps, the friction coefficient will increase to the maximum 10.2. With increasing the sliding time, the friction coefficient decreases quickly and then be steady at about 1.75. Thus, the friction force is basically higher than the normal force at and the motion of upper substrate is seriously hindered.

The friction property analysis for rolling model with diamond nanoparticle at diameter of 35.7 Å, including the friction force, normal force and friction coefficient, are shown in the Figure 5. It can be seen that the friction force varying with the sliding time, which contains run-in period and stabilization period. When the sliding time is shorter than 65 ps, the friction force will be in the run-in period and it will increase when the sliding time is raised. But the friction force will be stable when the sliding time is more than 65 ps. The normal force fluctuates with 60.4 nN, which is close to the value of the external load (60 nN).

The similar property can also be found on the relationship between the friction coefficient and the sliding time. It also includes run-in period and stabilization period. When the average friction coefficient is in run-in period, the friction coefficient will increase with increasing sliding time. Also, the average friction coefficient will keep stable when it is in stabilization period. To explain the friction period, the average indentation depth varying with the sliding time is calculated. As the Figure 6 shows, the average indentation depth increases with increasing the sliding time from 0 ps to 65 ps. But the indentation depth will be generally steady

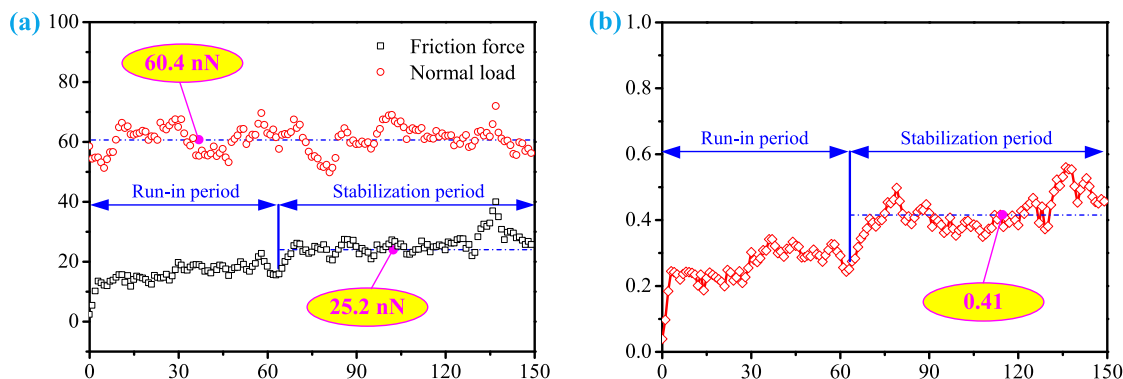


FIGURE 5. Friction property analysis for rolling model with diamond nanoparticle at diameter of 35.7 Å: (a) force and (b) friction coefficient.

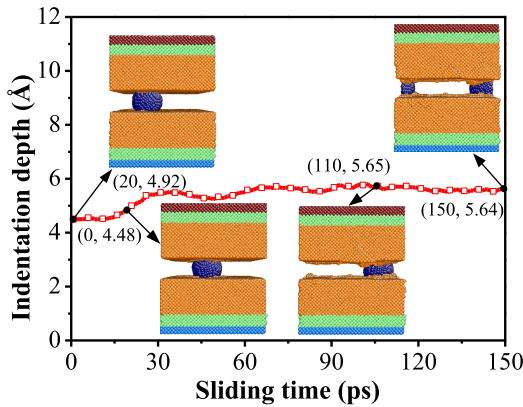


FIGURE 6. Indentation depth varying with the sliding time at diamond nanoparticle diameter of 35.7 Å.

when the sliding is larger than 65 ps. On the other hand, the friction morphologies at sliding time of 0 ps, 20 ps, 110 ps and 150 ps are given in Figure 6. The diamond nanoparticle are surrounded by copper atoms of substrate at 0 ps. But with increasing the sliding time, the number of atoms behind the nanoparticle decreases and more contact atoms are needed to produce the repulsive force to support the substrate, which increases the indentation depth. However, the number of diamond atoms surrounded by the copper atoms keeps constant in the stabilization period, so the indentation depth generally remains unchanged. As a result, the friction process can be divided into run-in period and stabilization period.

Comparing Figure 3 and Figure 5, it can be concluded that whether the diamond nanoparticle is added or not, there are the run-in period and stabilization period in the friction process. Unlike sliding model without diamond nanoparticle, both friction force and friction coefficient decrease with adding the diamond nanoparticle. In addition, the friction force and friction coefficient increases to the maximum and then decreases to the steady value in the sliding model, while they directly increases to the steady value in the rolling model. It can be concluded that the addition of diamond nanoparticle makes the friction process more stable and improves the friction reduction behaviors, which validates the friction reduction mechanism of diamond nanoparticle.

On the other hand, the diamond nanoparticle can roll when the upper substrate slides, which can change friction force and friction coefficient. To better explain the rolling property, the angular velocity of diamond nanoparticle is analyzed. The angular velocities whose rotate axis is z axis can indicate whether the diamond nanoparticle is rolling or not. The angular velocity at diamond nanoparticle diameter of 35.7 Å is shown in Figure 7. The angular velocity fluctuates with 0.028 rad/ps. When the sliding time is smaller than 65 ps, the angular velocity is in run-in period and it is in stabilization period at sliding time higher than 65 ps. On the other hand, the oscillating velocity is different at different sliding time. The oscillating velocity in the run-in period is higher than that in the stabilization period. The velocity oscillation can be considered to be from the atomic stepped

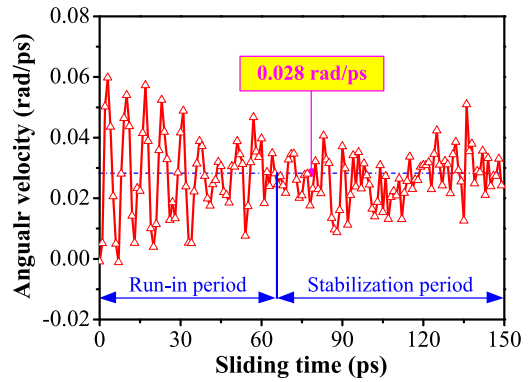


FIGURE 7. Angular velocity varying with the sliding time at diamond nanoparticle diameter of 35.7 Å.

surface of both the diamond nanoparticle and the substrate. Additionally, the angular velocity in run-in period sometimes becomes negative. Therefore, it can be concluded that the diamond nanoparticle have a tendency to roll with an oscillating velocity.

B. EFFECT OF DIAMETER ON THE INDENTATION PROPERTY

At same indentation depth, a larger size of the nanoparticle needs larger force, which means with same force, a larger size of the nanoparticle will result in smaller indentation depth [30]. Figure 8 describes the relationship between the indentation depth and the diameter of diamond nanoparticle. The initial indentation depth at sliding time of 0 ps is analyzed, which is shown in the Figure 8(a). It can be seen that the initial indentation depth (sliding time is 0 ps) reduces along with the diameter increase nonlinearly. To reveal the relationship between them, the curve fitting is adopted by the power function. It is predicted that the initial indentation depth inversely proportional to 3.6 power of the diameter. The correlation coefficient is 0.949.

Figure 8(b) shows the indentation depth varying with the sliding time for diamond nanoparticle with different diameters. No matter what the diameters are, all the indentation depths show the law of increasing first and then stabilizing. However, the fluctuation ranges of indentation depths are different at different diameters. The indentation depth at diameter of 49.98 Å is even higher than that at diameters of 42.84 Å and 46.41 Å at certain time. In addition, the final friction morphologies at diameters of 32.13 Å, 39.27 Å and 46.41 Å are shown in the Figure 9. The indentation is formed in the lower substrate at the friction process. The surface of lower substrate is totally destroyed at small diameter, such as 32.13 Å. However, the surface of upper substrate is basically not damaged at diameter of 46.41 Å. The result is coincident with the relationship between indentation depth and diameter in the Figure 8(b).

C. EFFECT OF DIAMETER ON THE FRICTION PROPERTY

Figure 10 shows a series of friction property with respect to sliding time at different diameter, including friction force,

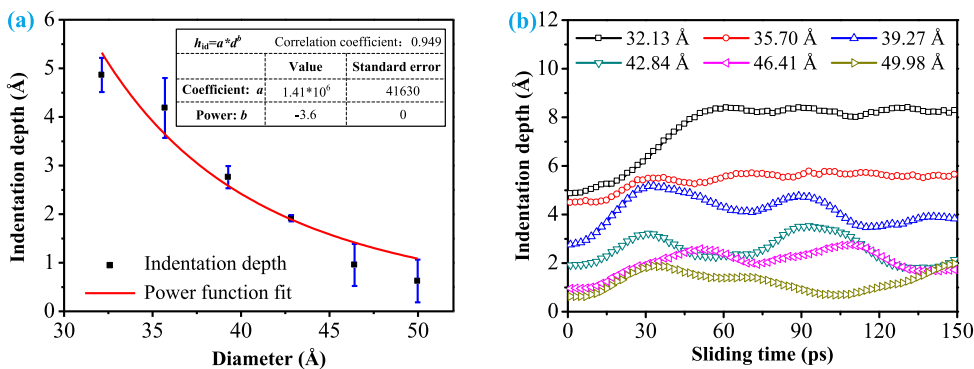


FIGURE 8. Relationship between the indentation depth and the diameter of diamond nanoparticle: (a) Initial indentation depth varying with diameter at sliding time of 0 ps and (b) Indentation depth varying with sliding time at different diameters.

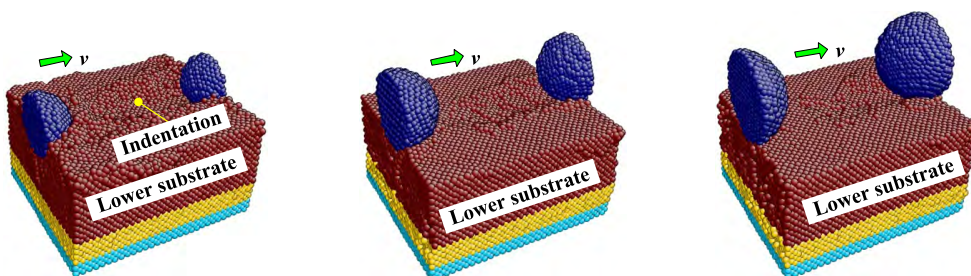


FIGURE 9. Final friction morphologies of lower substrate at different diameters: (a) $d=32.13 \text{ \AA}$, (b) $d=39.27 \text{ \AA}$, and (c) $d=46.41 \text{ \AA}$.

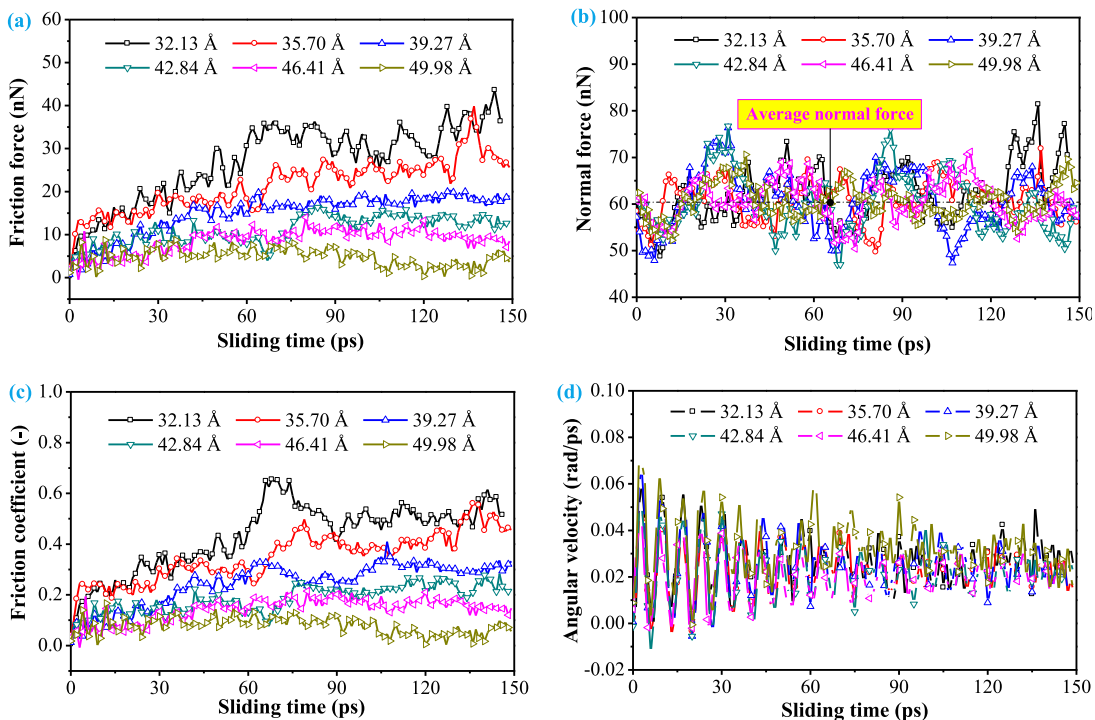


FIGURE 10. Effect of diameter on the friction property with respect to sliding time: (a) friction force, (b) normal force, (c) friction coefficient, and (d) angular velocity.

normal force, friction coefficient and angular velocity. As can be seen from Figure 10(a), all the friction forces with different diameters show the trend of first growth and then stability and

they can be divided into run-in period and stabilization period. For the diamond nanoparticle with large diameter (49.98 \AA), the friction force is negative at sliding time $100 \text{ ps} \sim 125 \text{ ps}$.

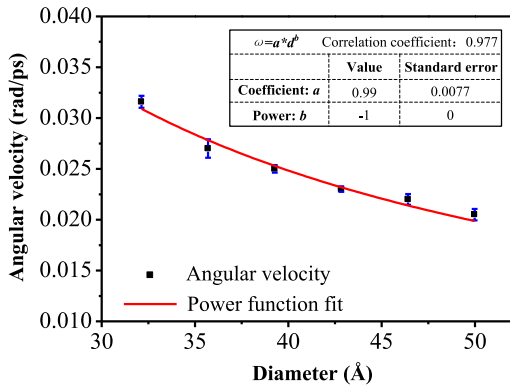


FIGURE 11. Effect of diameter on the average angular velocity of diamond nanoparticle.

This is mainly due to the random motion of the atoms. The number of contact copper atoms behind the diamond nanoparticle is even more than that in front of diamond nanoparticle at some point. The friction force will be negative and promote the motion of diamond nanoparticle. But when the diameter decreases, more atoms accumulate in front of the nanoparticle, which will raise the fluctuation range and average value of the friction force. So the friction force always prevents the motion for the diamond nanoparticle with small diameter.

Figure 10(b) illustrates the normal force varying with the sliding time at different diameter. The normal forces fluctuate with the average normal force and they have the same fluctuation range, no matter what the diameters are. It indicates that the normal force, including the fluctuation range and the average value, is irrelevant to the diameter. As shown in Figure 10(c), the relationship between the friction coefficient and the sliding time is similar to that of the friction force. The friction coefficient increases with decreasing the diameter. At diameter of 49.98 Å, the friction coefficient is even negative at 100 ps~125 ps. But when the diameter decreases, the friction coefficient increases gradually and this phenomenon disappears.

Figure 10(d) shows the effect of diameter on the angular velocity. The angular velocity fluctuates with the increase of sliding time at any diameters. The fluctuation range at run-in period is higher than that at stabilization period. However, the effect of diameter on the angular velocity is not obvious in the Figure 10(d). In order to describe the relationship between the angular velocity and the diameter more intuitively, the average angular velocity is calculated and the relationship between the average angular velocity and diameter is analyzed, which is shown in the Figure 11. The average angular velocity is inversely proportional to the diameter ($\omega = 0.99/d$) and the correlation coefficient

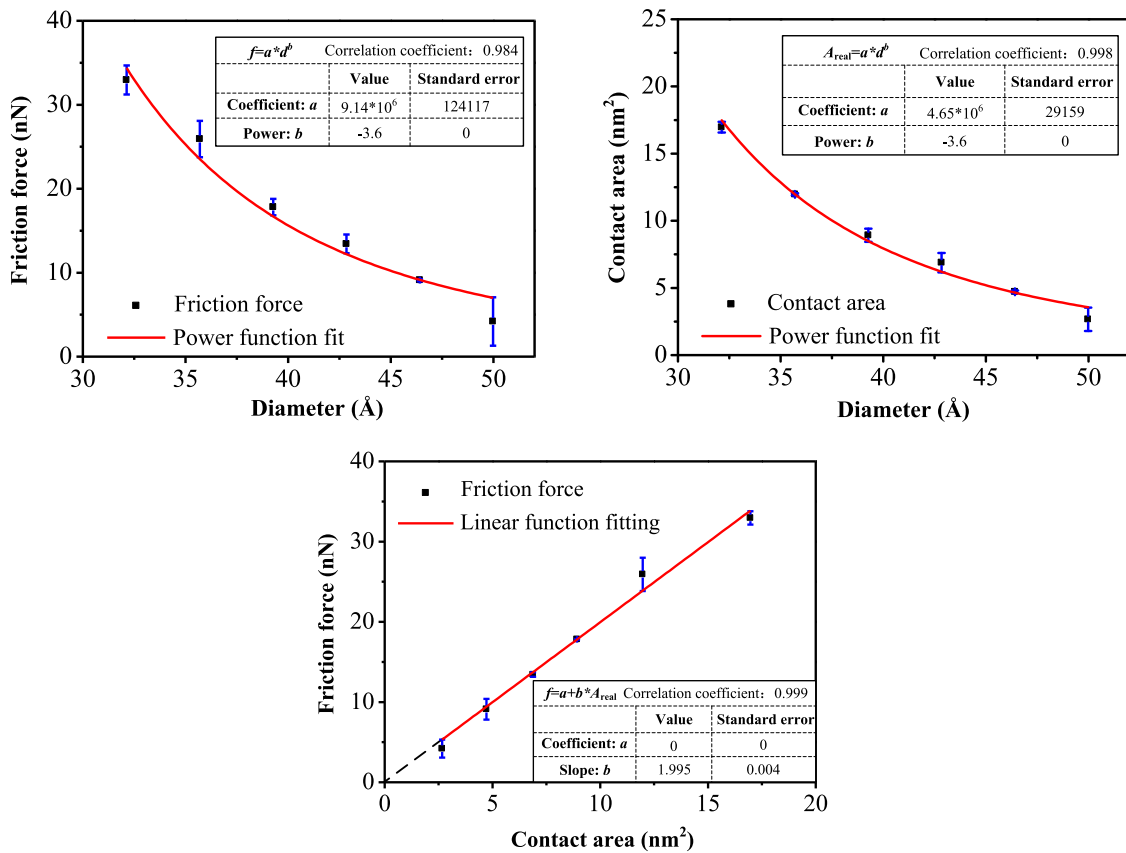


FIGURE 12. Mechanism of diameter changing the friction property: (a) relationship between friction force and diameter, (b) relationship between contact area and diameter, and (c) relationship between friction force and contact area.

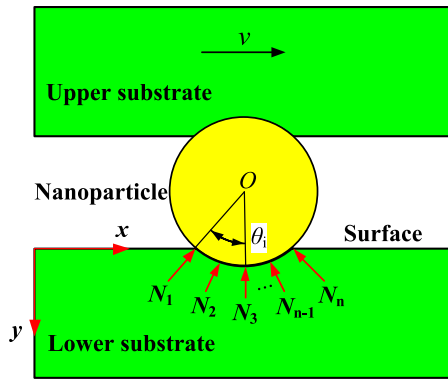


FIGURE 13. Force analysis of rolling model with diamond nanoparticle.

is 0.977. The power fit shows an excellent agreement with the formula.

To explain how the diameter of diamond nanoparticle changes the friction mechanism, the contact area is calculated and the effect of diameter on the friction force and contact area is analyzed, which is shown in the Figure 12. Figure 12(a) illustrates the friction force varying with the diameter. The friction force is inversely proportional to 3.6 power of the diameter and the correlation coefficient is 0.984. The nonlinearly decrease of friction force with the diameter indicates that the slope of the fitting curve decreases with the increase of diameter. The larger the diameter is, the more the increment magnitude of friction force increases.

Figure 12(b) described the effect of diameter on the contact area. It can be found that the contact area depends nonlinearly on the diameter. Considering that the friction force and the real contact area are both inversely proportional to the 3.6 power of the diameter, their relationship is fitted adopting the power function and the result is shown in the Figure 12(c). The fitting curve is a straight line across ordinate origin. As a result, the friction force is a linear function of the contact area. Therefore, it can be concluded that the diameter of diamond nanoparticle affects the friction force by changing the contact area.

To explain why the friction force depends nonlinearly on the diameter, a force analysis of rolling model with diamond nanoparticle is conducted, which is shown in the Figure 13. From the force analysis, it can be seen that the friction force and the normal force of lower substrate can be calculated by

$$\begin{cases} f = \sum_{i=1}^n N_i \sin \theta_i \\ F_N = \sum_{i=1}^n N_i \cos \theta_i \end{cases} \quad (5)$$

where N_i is force that the i diamond contact atom acting on the lower substrate and it points towards the center of the diamond nanoparticle. θ_i is the angle between N_i and y axis. The components of N_i in the x axis and y axis are the friction force and normal force, respectively. Assuming that the forces N_i are constant for the contact atoms, the closer to the surface of lower substrate, the larger the angle θ_i is. From Eq. (6),

it can be deduced that the atom closer to the surface generates higher friction force. According to the relationship between the indentation depth and the diameter, the indentation depth increases with decreasing the diameter. Thus, the number of contact atoms required for large diameter particle decreases drastically, which reduces the friction force rapidly.

IV. CONCLUSION

In this paper, the MD simulation was conducted to investigate the rolling friction property adopting the LAMMPS software. A sliding model with two substrates and a rolling model with two substrates and a diamond nanoparticle were built. In addition, effect of diameter on the friction property was also studied. The conclusions were drawn as follows:

(1) The friction force is higher than the normal force and the friction coefficient is greater than one in the sliding model without diamond nanoparticle. But when the diamond nanoparticle is added, the friction force and friction coefficient decreases obviously. Thus, the adding of diamond nanoparticle can improve the friction property. Additionally, the friction force and friction coefficient varying with sliding time consist of run-in period and stabilization period. Unlike the trend of increasing first and then decreasing to stable values in the sliding model, the friction force and friction coefficient increase to the stable values directly in the rolling model.

(2) In the sliding process of the upper substrate, the rolling phenomenon of the diamond nanoparticle is observed. The angular velocity fluctuates around the sliding time and the fluctuating range rises afterwards steady. On the other hand, the angular velocity will decrease inversely when the diameter of diamond nanoparticle is raised. The relationship between them is $\omega = 0.99/d$.

(3) In the model of rolling friction, the indentation depth firstly increases and then tends to be stable. With the increase of the diameter, the indentation depth decreases nonlinearly. The power relationship between the indentation depth and the diameter is $h_{id} = 1.41 \times 10^6 \times d^{-3.6}$.

(4) The diameter of diamond nanoparticle has an important effect on the friction property. As the diameter increases, both the friction force and the friction coefficient decrease nonlinearly. On the other hand, the relationship among the diameter, the friction force and the contact area is fitted. It is found that the friction force and the contact area show power relationship decrease with the diameter. The curve of friction force and contact area is a straight line ordinate origin. Therefore, it can be concluded the friction force is actually affected by the contact area.

REFERENCES

- [1] Z. Wan, X. Liu, H. Wang, and Y. Shan, "Research on the time-varying properties of brake friction (September 2018)," *IEEE Access*, vol. 6, pp. 69742–69749, 2018.
- [2] D. Wu, Y. Liu, D. Li, X. Zhao, and X. Ren, "The applicability of WC–10Co–4Cr/Si₃N₄ tribopair to the different natural waters," *Int. J. Refractory Met. Hard Mater.*, vol. 54, pp. 19–26, Jan. 2016.
- [3] H.-S. Kim, J.-W. Park, S.-M. Park, J.-S. Lee, and Y.-Z. Lee, "Tribological characteristics of paraffin liquid with nanodiamond based on the scuffing life and wear amount," *Wear*, vol. 301, nos. 1–2, pp. 763–767, 2013.

- [4] J. E. S. Dennis, K. Jin, V. T. John, and N. S. Pesika, "Carbon microspheres as ball bearings in aqueous-based lubrication," *ACS Appl. Mater. Interfaces*, vol. 3, no. 7, pp. 2215–2218, 2011.
- [5] H. Y. Chu, C. H. Wen, and J. F. Lin, "The anti-scuffing performance of diamond nano-particles as an oil additive," *Wear*, vol. 268, no. 7, pp. 960–967, 2010.
- [6] C. Novak, D. Kingman, K. Stern, Q. Zou, and L. Gara, "Tribological properties of paraffinic oil with nanodiamond particles," *Tribol. Trans.*, vol. 57, no. 5, pp. 831–837, 2014.
- [7] H.-J. Kim, K. H. Kang, and D.-E. Kim, "Sliding and rolling frictional behavior of a single ZnO nanowire during manipulation with an AFM," *Nanoscale*, vol. 5, no. 13, pp. 6081–6087, 2013.
- [8] S. Khokhriakov, R. R. Manumachu, and A. Lastovetsky, "Performance optimization of multithreaded 2D fast Fourier transform on multicore processors using load imbalancing parallel computing method," *IEEE Access*, vol. 6, pp. 64202–64224, 2018.
- [9] W. G. Lee, K. H. Cho, and H. Jang, "Molecular dynamics simulation of rolling friction using nanosize spheres," *Tribol. Lett.*, vol. 33, no. 1, pp. 37–43, 2009.
- [10] L. Zhang and H. Tanaka, "Atomic scale deformation in silicon monocrystals induced by two-body and three-body contact sliding," *Tribol. Int.*, vol. 31, no. 8, pp. 425–433, 1998.
- [11] J. Sun, L. Fang, J. Han, Y. Han, H. Chen, and K. Sun, "Phase transformations of mono-crystal silicon induced by two-body and three-body abrasion in nanoscale," *Comput. Mater. Sci.*, vol. 82, no. 3, pp. 140–150, 2014.
- [12] J. Sun, L. Fang, J. Han, Y. Han, H. Chen, and K. Sun, "Abrasive wear of nanoscale single crystal silicon," *Wear*, vol. 307, nos. 1–2, pp. 119–126, 2013.
- [13] L. Si, D. Guo, J. Luo, X. Lu, and G. Xie, "Abrasive rolling effects on material removal and surface finish in chemical mechanical polishing analyzed by molecular dynamics simulation," *J. Appl. Phys.*, vol. 109, no. 8, 2011, Art. no. 084335.
- [14] Y.-R. Jeng, P.-C. Tsai, and T.-H. Fang, "Molecular dynamics studies of atomic-scale friction for roller-on-slab systems with different rolling-sliding conditions," *Nanotechnology*, vol. 16, no. 9, p. 1941, 2005.
- [15] C. Hu, M. Bai, J. Lv, H. Liu, and X. Li, "Molecular dynamics investigation of the effect of copper nanoparticle on the solid contact between friction surfaces," *Appl. Surf. Sci.*, vol. 321, pp. 302–309, 2014.
- [16] C. Hu, M. Bai, J. Lv, Z. Kou, and X. Li, "Molecular dynamics simulation on the tribology properties of two hard nanoparticles (diamond and silicon dioxide) confined by two iron blocks," *Tribol. Int.*, vol. 90, pp. 297–305, Oct. 2015.
- [17] J. Shi, L. Fang, and K. Sun, "Friction and wear reduction via tuning nanoparticle shape under low humidity conditions: A nonequilibrium molecular dynamics simulation," *Comput. Mater. Sci.*, vol. 154, pp. 499–507, Nov. 2018.
- [18] A. V. Khomenko and N. V. Prodanov, "Study of friction of Ag and Ni nanoparticles: An atomistic approach," *J. Phys. Chem. C*, vol. 114, no. 47, pp. 19958–19965, 2010.
- [19] A. Khomenko, M. Zakharov, D. Boyko, and B. N. J. Persson, "Atomistic modeling of tribological properties of Pd and Al nanoparticles on a graphene surface," *Beilstein J. Nanotechnol.*, vol. 9, no. 1, pp. 1239–1246, 2018.
- [20] N. V. Prodanov and A. V. Khomenko, "Computational investigation of the temperature influence on the cleavage of a graphite surface," *Surf. Sci.*, vol. 604, nos. 7–8, pp. 730–740, 2010.
- [21] J. Shi, J. Chen, X. Wei, L. Fang, K. Sun, and J. Sun, "Influence of normal load on the three-body abrasion behaviour of monocrystalline silicon with ellipsoidal particle," *RSC Adv.*, vol. 7, no. 49, pp. 30929–30940, 2017.
- [22] S. Plimpton, *Fast Parallel Algorithms for Short-Range Molecular Dynamics*. New York, NY, USA: Academic, 1995.
- [23] J. Li, "AtomEye: An efficient atomistic configuration viewer," *Model. Simul. Mater. Sci. Eng.*, vol. 11, no. 2, p. 173, 2003.
- [24] M. S. Daw, S. M. Foiles, and M. I. Baskes, "The embedded-atom method: A review of theory and applications," *Mater. Sci. Rep.*, vol. 9, nos. 7–8, pp. 251–310, 1993.
- [25] J. Zhang, T. Sun, Y. Yan, Y. Liang, and S. Dong, "Molecular dynamics study of groove fabrication process using AFM-based nanometric cutting technique," *Appl. Phys. A*, vol. 94, no. 3, pp. 593–600, 2009.
- [26] W. Shi, X. Luo, Z. Zhang, Y. Liu, and W. Lu, "Influence of external load on the frictional characteristics of rotary model using a molecular dynamics approach," *Comp. Mater. Sci.*, vol. 122, pp. 201–209, Sep. 2016.
- [27] Y. Mo, K. T. Turner, and I. Szlufarska, "Friction laws at the nanoscale," *Nature*, vol. 457, no. 7233, pp. 1116–1119, 2009.
- [28] I. Szlufarska, R. K. Kalia, A. Nakano, and P. Vashishta, "A molecular dynamics study of nanoindentation of amorphous silicon carbide," *J. Appl. Phys.*, vol. 102, no. 2, 2007, Art. no. 023509.
- [29] Y. Mo and I. Szlufarska, "Roughness picture of friction in dry nanoscale contacts," *Phys. Rev. B, Condens. Matter*, vol. 81, no. 3, 2010, Art. no. 035405.
- [30] L. Yang and A. Martini, "Nano-scale roughness effects on hysteresis in micro-scale adhesive contact," *Tribol. Int.*, vol. 58, no. 2, pp. 40–46, 2013.



WEIJIE SHI received the B.S. degree in mechanical engineering from the Wuhan University of Technology, Wuhan, China, in 2012, and the Ph.D. degree in mechanical engineering from the Huazhong University of Science and Technology, Wuhan, in 2018. Then, he joined the College of Electromechanical Engineering, Qingdao University of Science and Technology, Qingdao, China, as a Lecturer. His current research interests include the material design of water hydraulics components and computational materials science.



HAIXIA ZHAO received the B.S. degree in mechanical engineering from Xi'an Shiyong University, Xi'an, China, in 1991, and the M.S. degree in mechanical engineering from the Qingdao University of Science and Technology, Qingdao, China, in 2007, where she is currently pursuing the Ph.D. degree with the College of Electromechanical Engineering. In 2000, she joined the College of Electromechanical Engineering, Qingdao University of Science and Technology, where she has been an Assistant Professor, since 2008. Her research interests include mechanical design and material science.



XIAOHUI LUO received the B.S. degree in mechanical engineering from the Wuhan University of Technology, Wuhan, China, in 2004, and the Ph.D. degree in mechanical engineering from the Huazhong University of Science and Technology, Wuhan, in 2009. From 2009 to 2011, he was a Postdoctoral Researcher with Ships and Marine Engineering, Huazhong University of Science and Technology. In 2011, he joined the School of the Mechanical Science and Engineering, Huazhong University of Science and Technology, where he has been an Assistant Professor, since 2015. His research interests include material design, electrohydraulic control systems, and ships operation and control systems.